Pergamon

0042-6989(94)00261-4

Vision Res. Vol. 35, No. 12, pp. 1699–1711, 1995

0042-6989/95 $9.50 + 0.00

Contour Integration Across Depth

ROBERT F. HESS,* DAVID J. FIELD†

Received 6 July 1994; in revised form 22 September 1994

In order to investigate the extent of the local connections subserving contour integration across depth, we measured performance for detecting the continuity of a path of Gabor elements distributed in depth and embedded in a three-dimensional field of random background elements. The results show that performance cannot be explained in terms of monocular performance and that contour information is not limited to single disparity planes. Path detection does indeed involve the integration of information across different, very disparate depth planes. The rules which emerge are in general similar to that already described in the two-dimensional case in as far as orientation and disparity are important. Unlike the two-dimensional case, three-dimensional integration operates over relatively large three-dimensional distances.

Contour integration Depth Association field

INTRODUCTION

Following from the early work on Gestalt grouping principles (e.g. Wertheimer, 1938) there has been continued interest into the rules of how local image features are grouped together to define objects. Recent research from both a computational (e.g. Zucker, Dobbins & Iversen, 1989) and a psychophysical perspective (for discussion see Field, Hayes & Hess, 1993) have explored how the visual system integrates across the outputs of feature selective units in the early visual system. One recent approach (Field *et al.*, 1993; Field, Hayes & Hess, 1995; McIlhagga & Mullen, 1995) presents observers with arrays of oriented elements in which a subset is grouped by one of several rules. It was found that when a subset of the elements were placed along a path, the subset could be easily detected within the array even when the angles along the path changed as much as 60 deg. By looking at the conditions under which the path was detected, a theory was presented regarding how the outputs of cortical cells might be integrated or "associated". The results of these studies have been interpreted in terms of an "association field" which describes the integration of the responses of the early visual filters across distance, symmetry, phase, orientation and color.

Using similar stimuli, Kovacs and Julesz (1993) have shown that a similar integration process may be involved in the perception of closure, Watamaniuk, McKee and Grzywacz (1995) have shown similar effects for motion, while Polat and Sagi (1993) has shown that the relative alignment of neighboring elements can even effect the contrast threshold of elements at least when they are collinear.

In the current investigation we investigate whether the orientation and distance dependent interactions which form the basis of the postulated "association field" can be extended from the two-dimensional (2-D) to the three-dimensional (3-D) domain. In asking this question we want to resolve whether the outputs of orientationally-selective monocular and binocular cortical cells are linked in a similar way to define objects. Two factors make this seem likely. Firstly, the locus of binocularity is early in the primary visual cortex and is likely to precede the later computations of continuity. Second, everyday vision depends on defining objects in both 2-D and 3-D via rules of continuity and it would seem reasonable to have common rules of association which could be applied to objects spanning distances within the one plane as well as across different planes. On the other hand, there is psychophysical evidence that stereoscopic mechanisms are orientationally unselective (Mayhew & Frisby, 1978; Akerstrom & Todd, 1988, but also see Mansfield & Parker, 1994).

Our initial expectation on the basis of our previous 2-D studies (Field *et al.*, 1993, 1995) was that contour integration would only hold over small 3-D distances and decrease with increasing disparity. We expected to be able to define a 3-D association field for contour integration in depth. However, as described below, we found that the subjects could integrate the elements along a path even when the elements were at quite large disparities. This surprising result led to a series of studies on the mechanism involved in integrating these large disparities. The studies below show that although we are clearly dealing with a binocular, oriented mechanism, the integration across mechanisms appears to be almost unselective to disparity. In the following studies, stimuli

*Department of Ophthalmology, McGill Vision Research, McGill University, 687 Pine Avenue West, Montreal, Quebec, Canada H3A 1A1 [*Fax* 1 514 843 1691].

†Department of Psychology, Cornell University, Ithaca, NY 14853, U.S.A.

are created which consist of arrays of Gabor functions where each element occurs in one of two depth planes. In all cases, the disparity between the two depth planes is relatively large. As in our previous study (Field *et al.*, 1993) the subjects are asked to determine whether the array contains a subset of elements that are aligned along a path. By manipulating the properties of the elements, these studies explore how the visual system integrates across 3-D distances.

METHODS

In all experiments the observers' task was to identify the "path stimulus". A path stimulus consisted of a set of oriented Gabor elements aligned along a common contour, embedded in a background of similar, but randomly oriented Gabor elements. A no-path stimulus consisted of just randomly placed and randomly oriented Gabor elements. Gabor elements were used to control the spatial frequency composition of the stimuli so that the path could not be extracted by a single broad band detector. By using such stimuli we hope to gain a better understanding of the combinatorial rules which govern the outputs of visual neurones used in the extraction of the path from the background elements.

Stimuli

Two different types of bandpass elements were used in this study: oriented and non-oriented. The oriented Gabor elements were defined by the equation

$$g(x,y,\theta) = C \cdot \sin(2\pi f \cdot (x\sin\theta + y\cos\theta)) \exp\left(-\frac{x_2 + y^2}{2\sigma^2}\right) \quad (1)$$

where θ is the element orientation, for 0 to 360 deg, (x,y) is the distance in degrees from the element centre, and c is the contrast. The sinusoidal frequency f was 1.9 or 5.7 c/deg, the space constant σ was 0.26 or 0.08 deg respectively. The contrast was 35%.

The non-oriented elements were defined by the equation

$$g(x,y) = c \cdot \cos\left(2\pi\frac{R}{P}\right)\exp\left(-\left(\frac{R^2}{2\sigma^2}\right)\right) \quad (2)$$

where c is the contrast, $R = (\sqrt{x^2 + y^2})$, P is the spatial period of the sinusoid and σ is the space constant.

A no-path stimulus [see Fig. 1 (B)] was constructed in the following way. For the 5.7 c/deg condition, a 4.16 deg wide square was divided into a 8×8 grid of equally sized cells. A Gabor element of random orientation was placed in each display cell, with the restriction that each cell contain the centre of only one Gabor element. This eliminates the clumping of elements due to random placement. The elements were also placed to avoid overlap as much as possible. Once an empty cell was chosen, its neighbours were examined to see if they contained a Gabor element. If this is not the case a background element was laid down at some random point within the cell. If one or more of the neighbours contained a Gabor element then the new element was laid down at a position within the cell to avoid overlap. If this was impossible it was laid down in a position within the cell to minimize overlap. Usually there were fewer than two element overlaps per image.

A path stimulus consisted of two parts; the path itself [Fig. 1 (A)] and the background [Fig. 1 (B)]. The construction of the path is illustrated in Fig. 2. The path had a background of six invisible line segments; each line segment was of length 0.62 deg ($\pm$a step jitter) and the line segments joined at an angle uniformly distributed from $\alpha - 10$ to $\alpha + 10$ deg. α is called the path angle. Gabor elements were then placed at the middle of each line segment. The orientation θ of each element was the same as the orientation of the line segment on which it was placed. A ± 10 deg randomly selected off-path rotation was selected about angle θ, this was termed element_angle jitter. The orientation of each line segment was ambiguous (within the range 0–360), but traversing the path from one end to the other imposes a direction (and hence an unambiguous orientation) on each of the component line segments. Finally to avoid random changes in path detection due to random path closure which can have significant effects on path detection (Kovacs & Julesz, 1993), the path was checked to ensure that it neither intersected itself, nor looped back on itself. If so it was discarded and a new path generated.

The entire path contour was pasted into the display at a random location, ensuring that the centres of the Gabor elements occupied different cells. Finally, empty cells were filled with randomly oriented Gabor elements, as described in the no-path stimulus above. The average length of each backbone line segment (0.62 deg) was the same as the average distance between neighbouring Gabor elements in the background. Previous studies (Field *et al.*, 1993; McIlhagga & Mullen, 1995) have shown that path detection varies inversely with the length of the backbone line segments, but in a smooth manner, so the choice of segment length was not critical.

Neither the local or the global element density served as a cue to detection of path from no-path stimuli. The average distance from an element to its neighbour was no different for path and no-path stimuli. Secondly, the total number of empty cells were the same for path and no-path stimuli. If element density is not a cue then path detectability should be solely due to the alignment of elements in the path, since nothing else distinguishes path from no-path stimuli. McIlhagga and Mullen (1995) confirmed this in a control experiment where orientation of the path elements was randomized; they found that the path could not be detected, even under extended viewing conditions, regardless of the path angle α. We also conducted a control with non-oriented elements distributed across depth (Fig. 9) with similar conclusions.

Stereo-images

Stereo-images pairs each of 4.16×4.16 deg angular subtense, were generated and displayed on the monitor. These were binocularly combined with a mirror (four

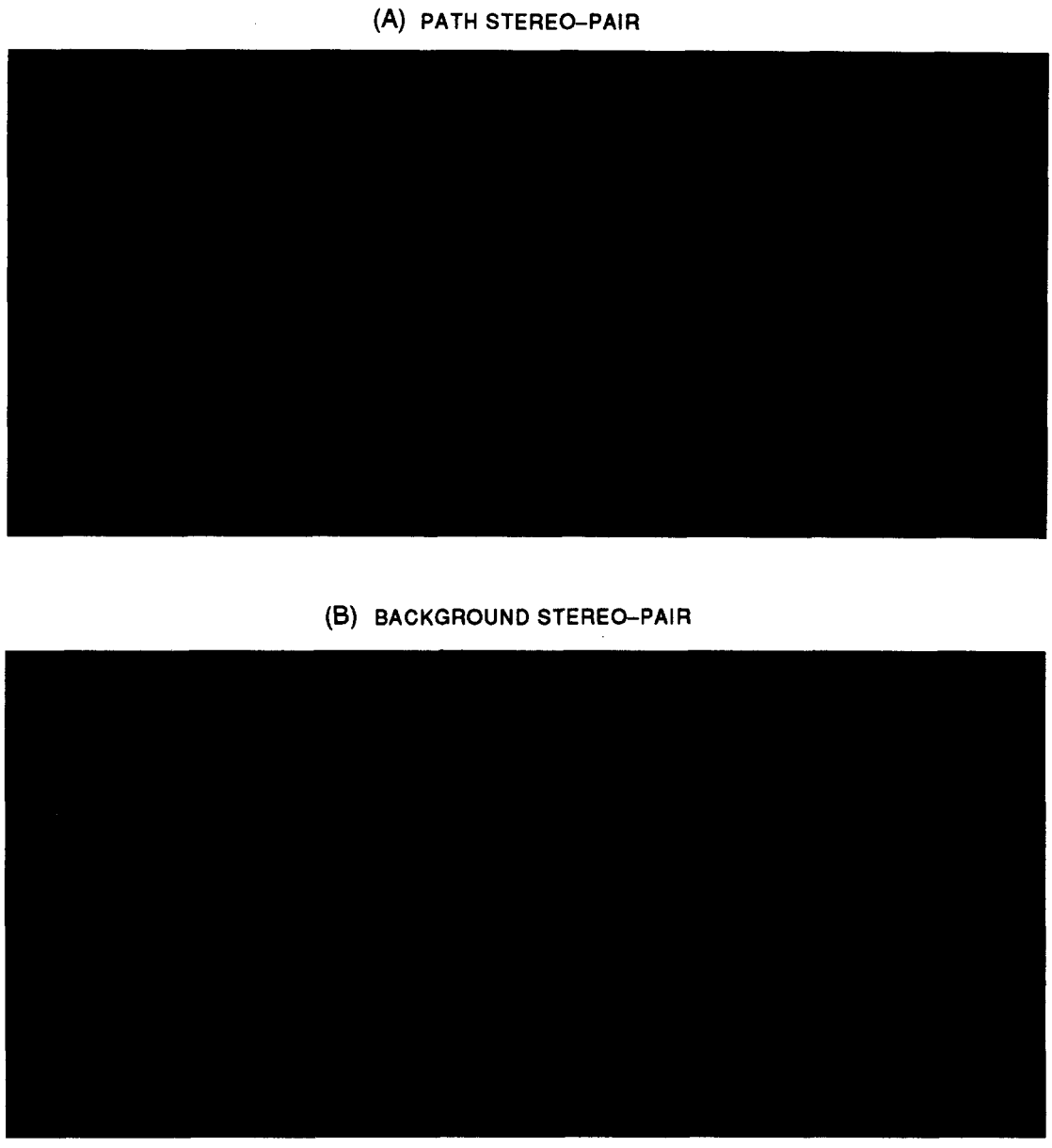

FIGURE 1. A path devoid of random background elements is displayed in (A). The background elements are displayed in (B). On each trial subjects were presented with equal probability with either the path + background elements or the background elements alone.

sets of two mirrors set at 90 deg to one another) haploscope. In principle, any element whether it be a path element or a background element could be displayed with an arbitrary disparity within the limits imposed by the size of the images and the overall display size. Disparities were produced by adding equal and opposite horizontal shifts to the elements in each stereo-pair. In practice, we limited these to only two depth planes on either side of the fixation plane which was defined by a nonious marker to ensure stable convergence. Each stereo-image pair contained an abrupt luminance border which facilitated fusion within the plane of the screen. The perception of elements in depth was strong and once initiated maintained itself for each of the brief presentations within each block of trials. Each alternate path element had a disparity ($\pm$a depth_jitter) associated with plane 1 while other path elements had a disparity ($\pm$a depth_jitter) associated with plane 2. This is diagrammatically illustrated in Fig. 3 for the path alone. The background elements were distributed in depth in exactly the same way as the path elements. The Appendix details the stimulus parameters used. Figure 5 shows a stereo-pair of the path stimulus.

Apparatus and experimental procedures

All stimuli were displayed on a Sony Trinitron monitor driven by a Sun Sparc station 2 computer, which generated stimuli on-line and controlled display and data collection. The mean luminance was 35 cd/m^2. The monitor was driven out by an 8-bit D/A converter and an 8-bit frame buffer. The monitor was gamma corrected in software. The gamma corrected monitor behaved linearly when displaying high spatial frequencies (12 c/deg square wave) up to 50% contrast. The monitor

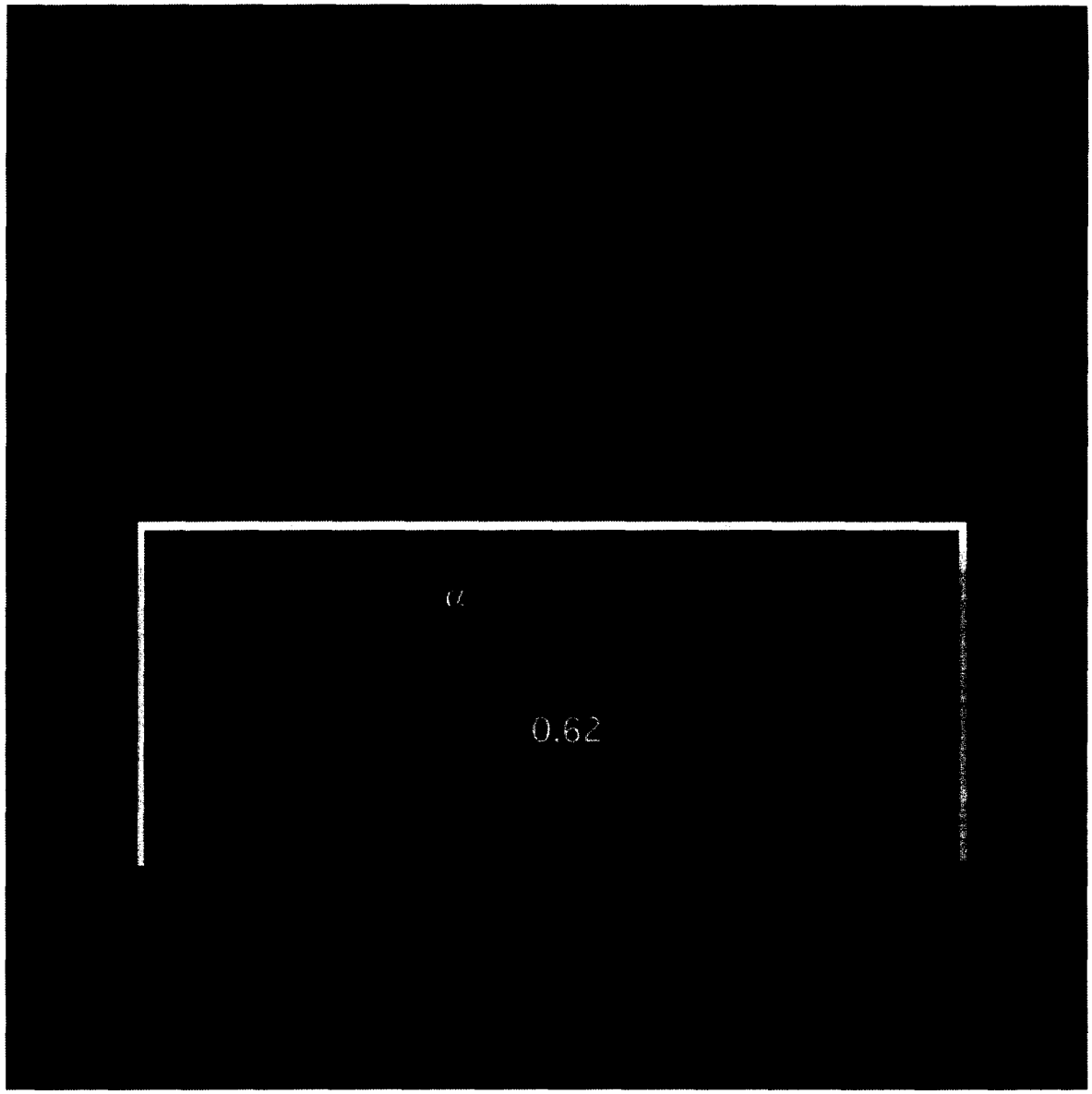

FIGURE 2. Path construction.

was viewed in an otherwise dark room through a four-mirror haploscope whose equivalent optical path was 130 cm. Each experimental run consisted of a block of 25 path stereo-images and 25 no-path stereo-images, randomly interleaved. In each run, the path angle α was set to 0, 5, 10, 20, 30 and 40 deg etc. Each presentation was cued to a "beep" and the subject had to decide whether the stimulus presentation, which was of 1 sec duration, contained a path or not. These stimuli give an instantaneous and vivid stereopercept in which a path oscillating between two depth planes is embedded 3-D noise. Typically, each block was repeated five times to obtain at least 250 trials per path angle. Thresholds were derived by fitting an error function to the psychometric data. This function had the form

$$y(x) = A \cdot (0.75 + 0.25 \cdot \mathrm{erf}((x - B)/(\sqrt{2} \cdot C))) \quad (3)$$

where A is the number of trials, B is the centring of the function and C is the standard deviation of the assumed underlying normally distributed error.

RESULTS

Our previous results have defined the association field for 2-D continuity (Field *et al.*, 1993, 1995). The first step towards investigating whether similar rules apply for paths defined in 3-D must involve assessing the contribution of purely monocular processes. For example, the monocular information may be sufficient to detect paths which are defined and perceived in depth. In the first experiment (Fig. 4) we address this issue by comparing monocular, binocular and stereoscopic performance for detection of paths of varying degree of jaggedness

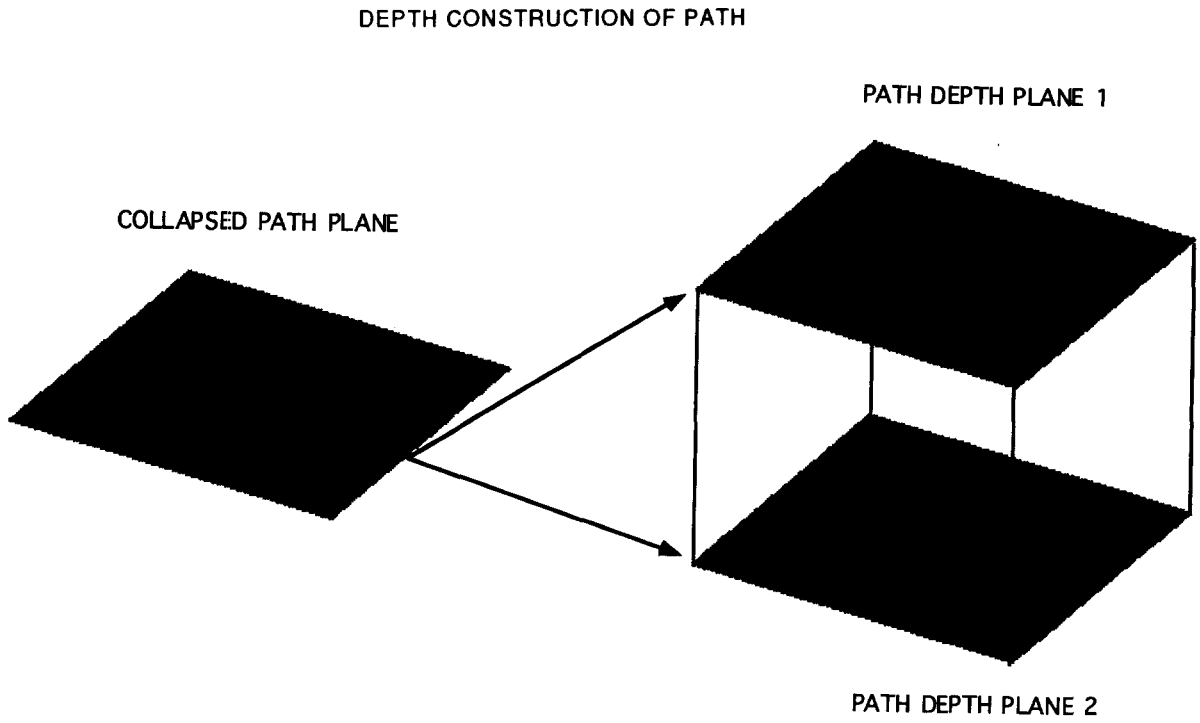

FIGURE 3. A path devoid of random background elements is displayed. The path elements are distributed in two different depth planes (planes 1 and 2). The equivalent 2-D representation is shown on the left.

(specified by path angle). In the binocular case (no-depth), the path and background elements are all in the plane of fixation. In the stereoscopic case, alternate path elements are in one of two depth planes (see Fig. 3 for illustration) which straddle the plane of fixation, with the background elements equally distributed in the two planes. The non-stereoscopic viewing case involves either monocular viewing of one of the images of the stereo-image pair [Fig. 4 (B)] or binocular viewing of one of the images of the stereo-image pair [Fig. 4 (A)]. The latter case corrects for probability summation when two eyes are used to view one of the monocular images.

Performance in terms of percent correct is plotted in Fig. 4 as a function of the jaggedness of the path, specified in terms of path angle (see Fig. 2 for definition). The results show that while performance is comparable for the binocularly fused (single plane of zero disparity) and stereoscopic (two depth planes) stimuli, it is reduced when viewing either members of the stereo-pair. This is true regardless of whether one of the stereo-pairs is

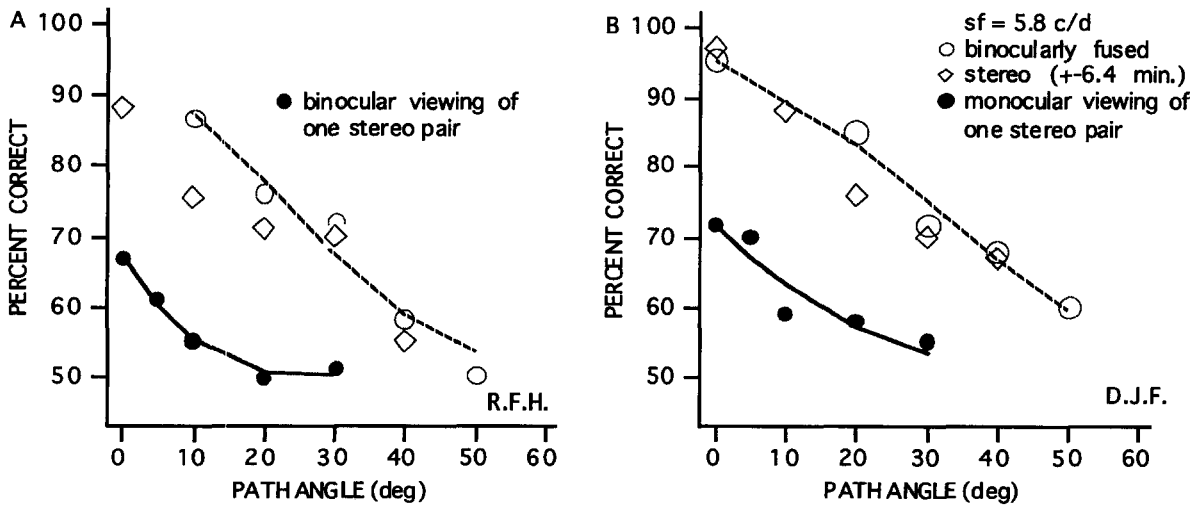

FIGURE 4. Psychometric performance is plotted for detection of signal paths as a function of the jaggedness of the path (path angle). Element spatial frequency is 5.8 c/deg. Results are displayed for two experienced psychophysical observers [(A) and (B)]. ○ Path detection in binocularly fused stereograms having zero disparity. ◇ Similar performance for the case where alternate path elements and half the background elements are distributed in one of two different depth planes. ● Performance using one of the monocular stereo image-pairs. In (A), one of the stereo-image pairs is viewed binocularly, whereas in (B) it is viewed monocularly. The curves are best fitting solutions to the data using equation (3). Note that path detection across two depth planes is as good as in the zero disparity plane and neither can be accounted for by using purely monocular information.

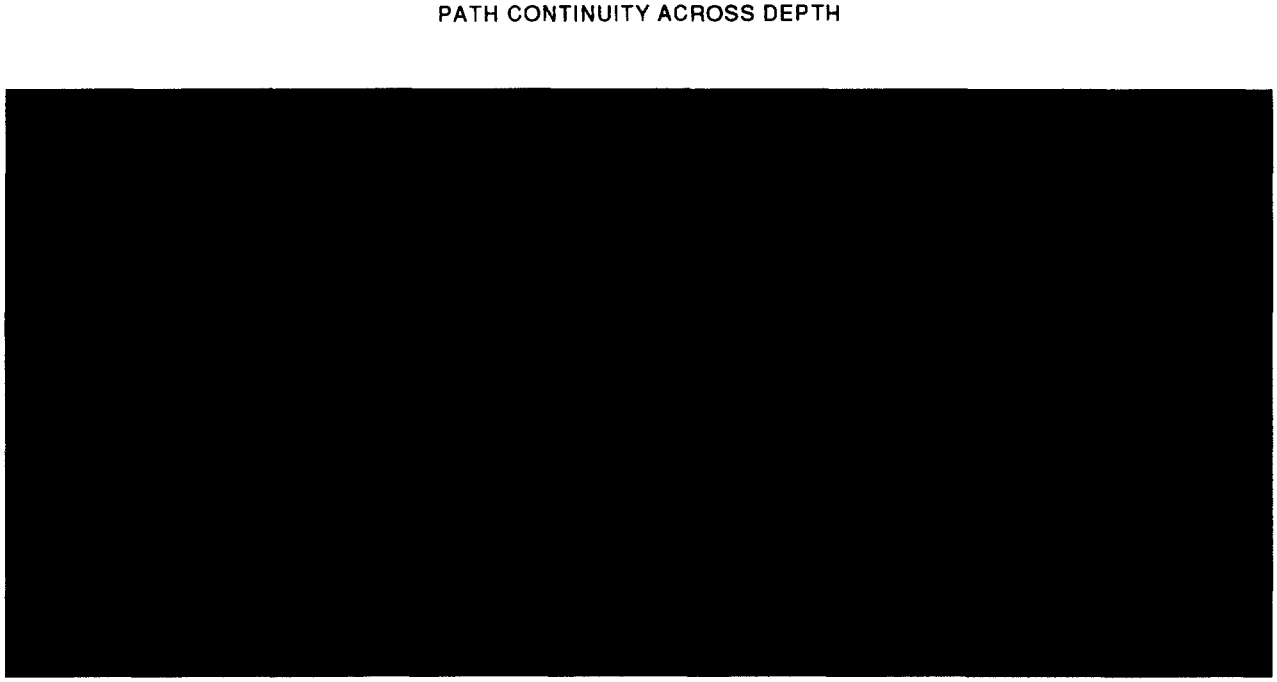

FIGURE 5. A stereo image-pair for investigating 3-D continuity as in the present experiment. Here the path angle is 10 deg and the disparity is ±6.4 min arc.

viewed monocularly, as for subject DJF [Fig. 4 (B)] or binocularly, as for subject RFH [Fig. 4 (A)]. The reason for the reduced performance and increased variability in the monocular case stems from the fact that, because of the depth oscillations in the path, alternate path elements in the monocular images are subject to a relatively large displacement either lateral to the path or along the path. It is this which disrupts monocular performance (Field *et al.*, 1993) which the reader can demonstrate for him/herself by comparing the binocular and monocular views of the demonstration provided in Fig. 5.

Thus the stimuli used here can be regarded as cyclopean in the special sense that binocular performance cannot be explained solely on the basis of monocular processing. Paths defined for purely binocular stimuli can be discriminated and their dependence on path angle has a comparable form to that found for monocular images using a comparable procedure (McIlhagga & Mullen, 1995; Field *et al.*, 1993, 1995).

The two depth planes in the previous stereoscopic condition were separated relative to the plane of fixation by ±6.4 min arc. In Fig. 6 we show how performance

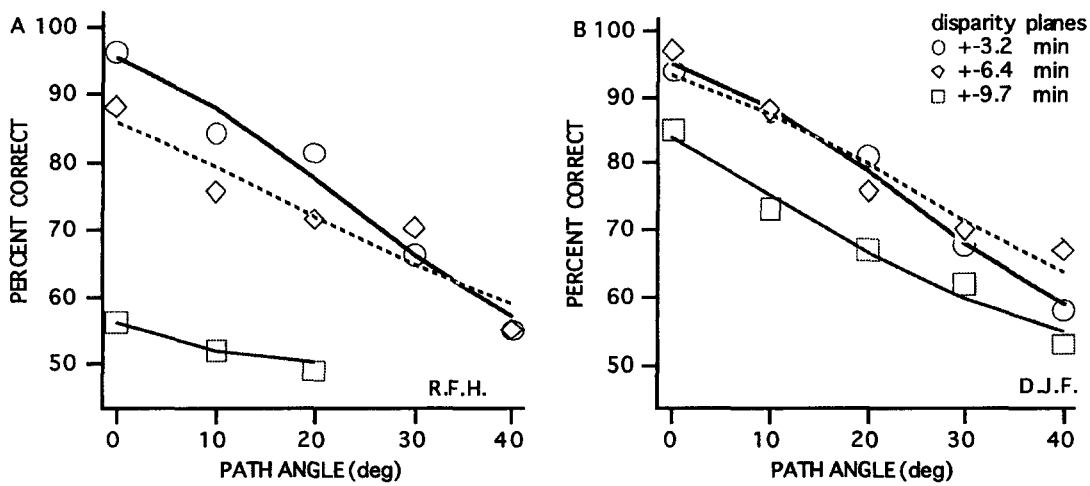

FIGURE 6. Psychometric performance is plotted for detection of signal paths as a function of the jaggedness of the path (path angle). Element spatial frequency is 5.8 c/deg. Results are displayed for two experienced psychiophysical observers [(A) and (B)]. ○ Path detection in stereograms where alternate path elements and half the background elements are distributed in one of two different depth planes having ±3.2 min arc disparity. ◇ Similar performance for a two plane disparity of ±6.4 min arc. □ Disparity planes of ±9.7 min arc. Each curve is the best fitting solution to the corresponding data using equation (3). Note that path detection across two depth planes is similar up until 6.4 min arc for these stimuli, after which it falls off.

for two observers varies as a function of path angles for a range of disparities (±3.2 to ±9.7 min arc) between the two planes. The element spatial frequency was unchanged at 5.8 c/deg. Disparities up to ±6.4 min arc give similar performance whereas performance deteriorates for higher disparities. In the disparity range above ±10 min arc, the quality of the depth percept deteriorates. For these stimulus parameters, above ±13 min arc there is no depth perceived in the display. The same dependence on path angle is seen for both observers for stimuli distributed across a large fraction of the available disparity range subserving depth perception.

Figure 7 displays similar results for stimulus elements a factor of 3 larger (spatial frequency = 1.9 c/deg). All aspects of the display were spatially scaled by changing the viewing distance. Results are shown for one observer, comparing binocular viewing without disparity, two magnitudes of disparity (±9.6 and ±19.2 min arc) and binocular viewing of one of the monocular-image pairs. Similar, though spatially scaled, results were obtained to those already described in Figs 4 and 6.

Does contour integration occur between or across depth planes? In the disparity range where performance was optimal, the percept was of a path whose elements alternately oscillated between two depth planes embedded in similar but randomly oriented background elements occupying the same two depth planes (see Fig. 5 for demonstration). This in itself does not constitute proof that the path information is being integrated

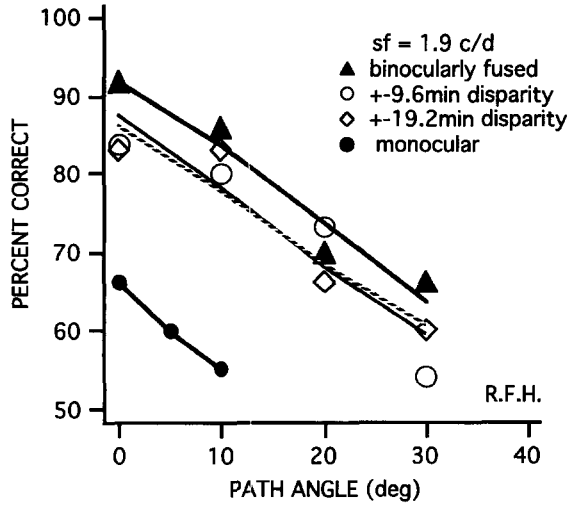

FIGURE 7. Psychometric performance is plotted for detection of signal paths as a function of the jaggedness of the path (path angle). Element spatial frequency is 1.9 c/deg. Results are displayed for one experienced psychophysical observer. ▲ Performance for the case where the images are binocularly fused and at zero disparity. ○ Path detection in stereograms where alternate path elements and half the background elements are distributed in one of two different depth planes having ±9.6 min arc disparity. ◇ Similar performance for a two plane disparity of ±19.2 min arc. ● Performance when one of the monocular-image pairs (±19.2 min arc disparity) is binocularly viewed. Each curve is best fitting solution to the corresponding data using equation (3). Note that path detection across two depth planes is similar up until ±19.2 min arc at this spatial frequency and that performance cannot be accounted for using purely monocular information.

between the two available depth planes. For example, the correspondence between performance within one plane in the binocularly fused case and between two planes in the disparity case (Fig. 4) can be adequately explained by assuming that continuity operations are limited to one depth plane at a time. In each case the signal-to-noise ratio of the path to background elements are the same because, in the disparity case within each plane, there are half the number of path, *and* background elements. Thus the present results argue for continuity computations within different depth planes but not necessarily *between* different depth planes. To make the case for "between depth planes" association field one needs to show that performance in the disparity task can be disruption by rendering the continuity information unusable within one of the two depth planes between which the path oscillates.

One way of testing whether the information in both depth planes is being used to solve for the path is to switch off all the elements (path and background) in one depth plane. If the information from only one depth plane is being used then performance should be unimpaired when one of the two planes is switched off. When this is done [Fig. 8 (A) ⧗] performance is dramatically reduced compared with the situation where elements occupy both planes [Fig. 8 (A) ○]. This suggests that in the two plane case, performance is governed by information across *both* depth planes. Another way of addressing this same issue of whether information is being used within or across depth planes is to subject the path elements in only one plane to a relatively large off-path orientation, since Field *et al.* (1993) have shown that there is only weak continuity for paths comprised of elements rotated by even moderate angles (e.g. 30 deg) off the axis of the path. In Fig. 8 (A and B) performance is compared for paths oscillating between two depth planes (for one observer they were ±3.2 min arc whereas for the other observer they were ±6.4 min arc). In one case (○), the off-path angle was randomly chosen between ±10 deg for each depth plane, whereas in the other case (●), it was 10 deg in one depth plane (randomly chosen from run to run) and 90 deg in the other depth plane. Performance is dramatically reduced by this manoever which renders the continuity information unusable in one of the two planes. This result also suggests that in the previous disparity tasks described above, information is indeed being integrated across the two available depth planes to solve for continuity. Furthermore, there appears to be no loss of efficiency in doing these computations either within one plane (binocularly fused case; Fig. 4) or across two depth planes (±3.2 and ±6.4 min arc disparity cases in Fig. 4 for stimuli of 5.8 c/deg; or ±9.6 min arc disparity case in Fig. 7 for stimuli of 1.9 c/deg).

Is orientation important for contour integration across depth? One of the conditions (●) displayed in Fig. 8 involved the case where alternate elements were rotated away from the path. This had a dominant effect on integration and suggests that element orientation is important in the linking of image features across depth.

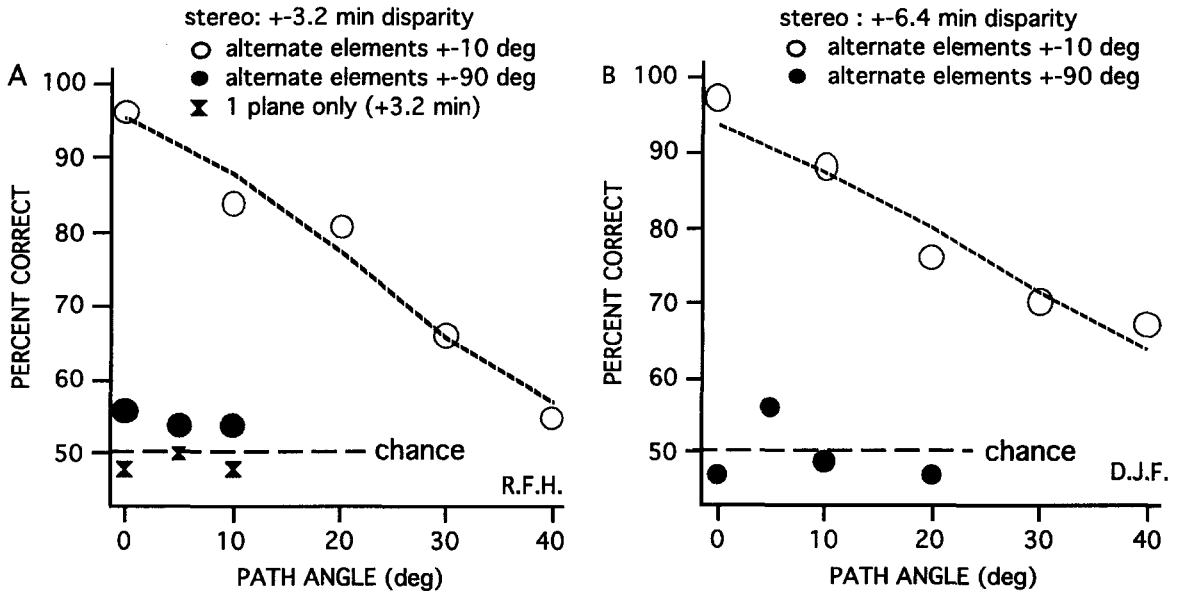

FIGURE 8. Psychometric performance is plotted for detection of signal paths as a function of the jaggedness of the path (path angle). Results are displayed for two experienced psychophysical observers [(A) and (B)]. ○ Path detection in stereograms where alternate path elements and half the background elements are distributed in one of two different depth planes having ±3.2 min arc (A) or ±6.4 min arc (B) disparity (off-path orientation is ±10 deg). ● Performance for a similar task except that the elements in one plane have a large off-path orientation (±90 deg). ⧗ Performance when all the elements (path and background) in one of the two depth planes are turned off. Each curve is best fitting solution to the corresponding data using equation (3). Note that by rendering the path information unusable in one plane either by turning them off [⧗ (A)] or by orienting them off the path backbone [● in (A) and (B)], performance deteriorates, indicating that in the baseline condition [○ in (A) and (B)] path information was being integrated across both depth planes.

This is further supported by comparing performance across two depth planes in the special cases where all the elements are oriented exactly orthogonal to the path [Fig. 9 (A) △]. In this case performance is not even above chance for perfectly straight paths (path angle of 0). There is a unique solution for defining the path in the case of the orthogonal element orientation. Since the observers had knowledge of how the path was constructed,

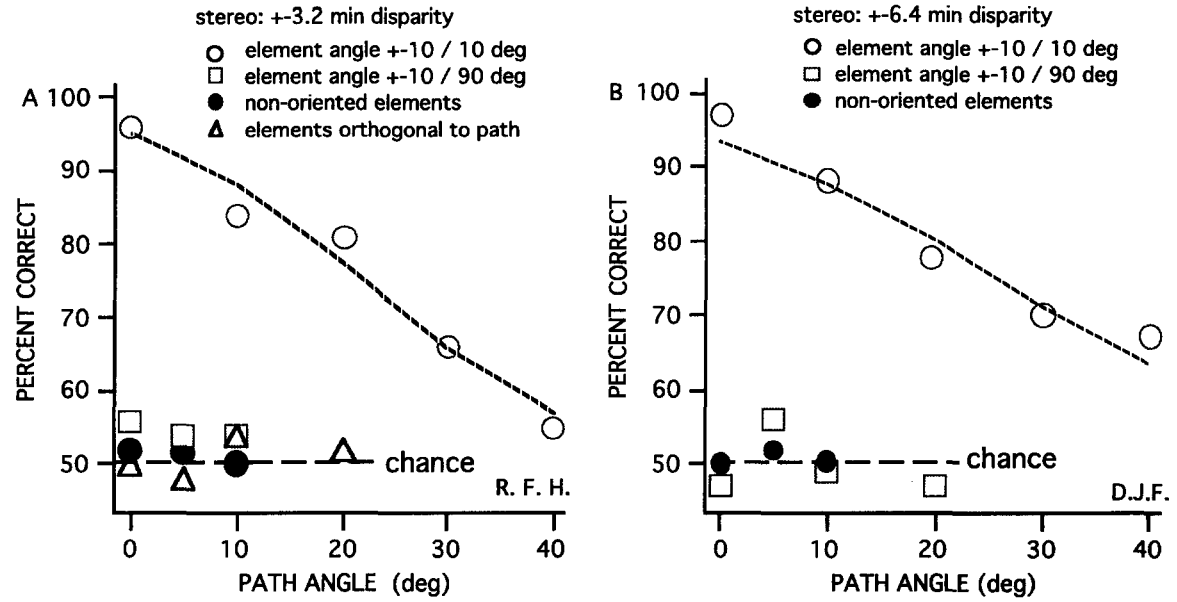

FIGURE 9. Psychometric performance is plotted for detection of signal paths as a function of the jaggedness of the path (path angle). Results are displayed for two experienced psychophysical observers [(A) and (B)]. ○ Path detection in stereograms where alternate path elements and half the background elements are distributed in one of two different depth planes having 3.2 min arc (A) or ±6.4 min arc (B) disparity. In each plane the elements have a ±10 deg randomly selected off-path jitter. Performance for the same task except that the elements are now non-oriented (Gaussian-weighted, sinusoidal bull's eyes). □ The case where the path elements in one depth plane have a large off-path orientation (±90 deg) compared with the elements in the other depth plane (±10 deg). △ in (A) are for the case where the elements are oriented exactly orthogonal to the path in both depth planes. The curve is the best fitting solution to the data using equation (3). All three manipulations disrupt performance (see text) from the baseline condition (○ and ◇).

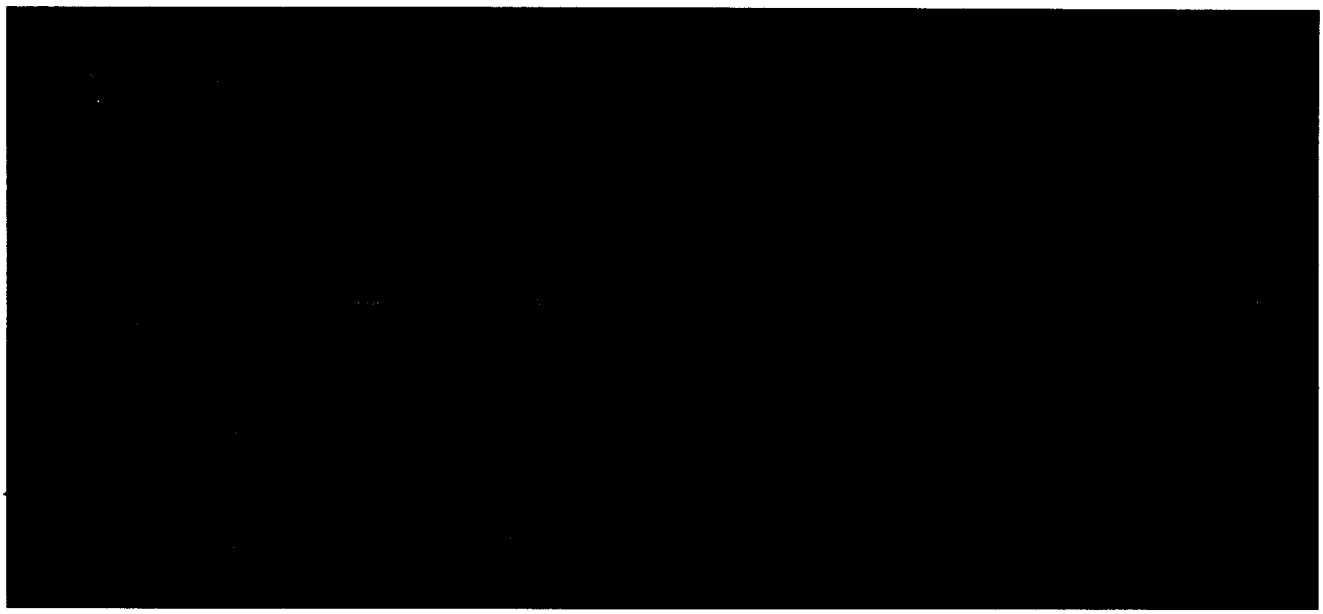

FIGURE 10. Stereo demonstration of path continuity between two depth planes in the case where the path is composed of orthogonally oriented elements. Such a maniupulation makes it difficult to see the path. Compare this with the demonstration in Fig. 3 where the conditions are similar except that now the elements are aligned along the path (±10 deg).

an ideal observer should show no decrement in performance for such a manipulation compared with the baseline condition in which all the path elements, within a 10 deg random variability, were aligned with the path. The fact that performance is dramatically reduced in this case highlights the importance of orientation for defining the 3-D association field, as was previously demonstrated to be the case for the 2-D association field (Field *et al.*, 1993). Figure 10 shows a stereo demonstration of our inability to integrate paths across two depth planes when the paths comprise orthogonally oriented elements. Compare this with the demonstration shown in Fig. 5 for paths comprised of aligned elements.

Figure 9 (●) also shows how performance is affected when non-oriented elements are used to construct path and background stimuli. In the non-oriented case, there is, of course, no unique solution to the path which is distributed across the two depth planes and for this reason it represents an important control for the presence of any local or global density cues (see Methods) which may artifactually facilitate detection of the path. Performance is at chance which suggests that such artifacts are not present.

How accurately do elements have to be aligned along the depth path? In Fig. 11, we see the dependence of path continuity on element off-path angle for two observers. The path angle in this experiment was set to 10 deg, ±10 deg of jitter and the two disparity planes were ±3.2 [Fig. 11 (A)] and ±6.4 [Fig. 11 (B)] min arc apart with random jitters of ±1.3 and ±2.6 min arc respectively. The dependence of performance on the off-path angle of the elements across depth is qualitatively similar to that already reported for monocular viewing (Field *et al.*, 1993). A detailed comparison is difficult because the numerous methodical differences between the two studies. However there appears to be less difference between changing the path angle versus the element angle (relative to the path) in the 3-D compared to the 2-D case.

DISCUSSION

The results of this study suggest that some of the rules of contour integration which have been previously considered only in terms of 2-D distances can be extended to 3-D distances. We have demonstrated that not only is monocular performance insufficient to explain the extraction of paths distributed between two depth planes but also that performance depends on the integration of contour information across *both* depth planes. These data therefore suggest that integration in these experimental conditions depends on associations between binocular units. In principle, such integration may occur either at fusion prior to stereopsis (Gillam, Chambers & Russo, 1988 but also see Methods/Stereo-images) or between binocular units over quite large disparities. This suggests that the integration process itself is not limited to binocular units that have similar disparities. What appears to be important to the association is the projected position and orientation of the units. That is, if we project the 3-D position of each element onto the horopter, then the integration is possible along similar constraints to the 2-D association field (Field *et al.*, 1993).

It should be noted that this leads to a curious problem. For an actual path that varies in 3-D, this alignment will

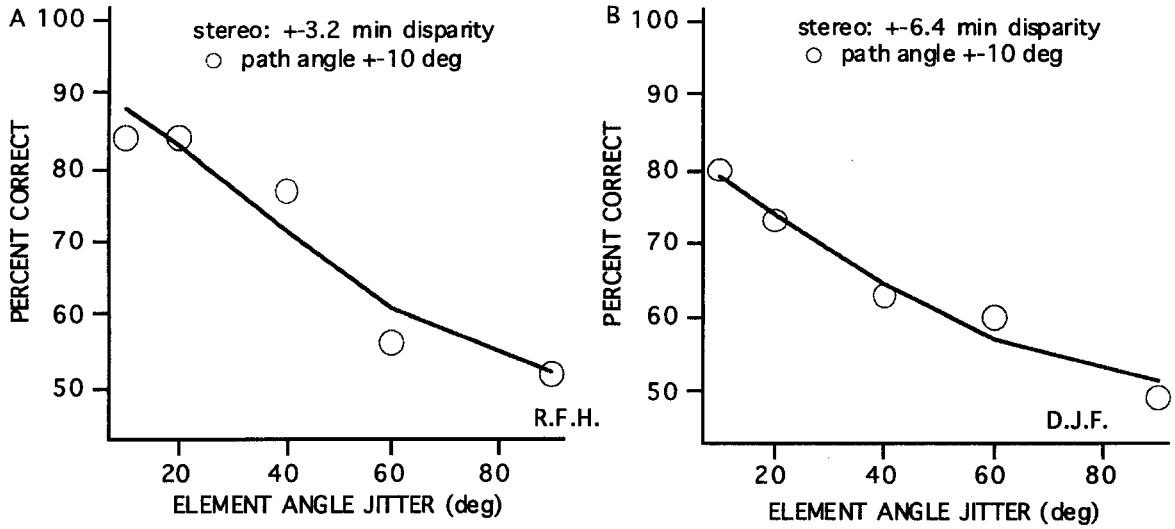

FIGURE 11. Psychometric performance is plotted for detection of signal paths as a function of the variability of the angle of a path element off the axis of the path (element angle). Results are displayed for two experienced psychophysical observers [(A) and (B)]. The path angle was 10 ± 10 deg of random off-path jitter. ○ Path detection in stereograms where alternate path elements and half the background elements are distributed in one of two different depth planes having ±3.2 min arc (A) or 6.4 min arc (B) disparity. The curve is the best fitting solution to the data using equation (3). This dependence across depth is qualitatively similar to that previously reported by Field *et al.* (1993) for the zero disparity plane.

A. CONTOUR DEFINED BY TEXTURE DEPTH

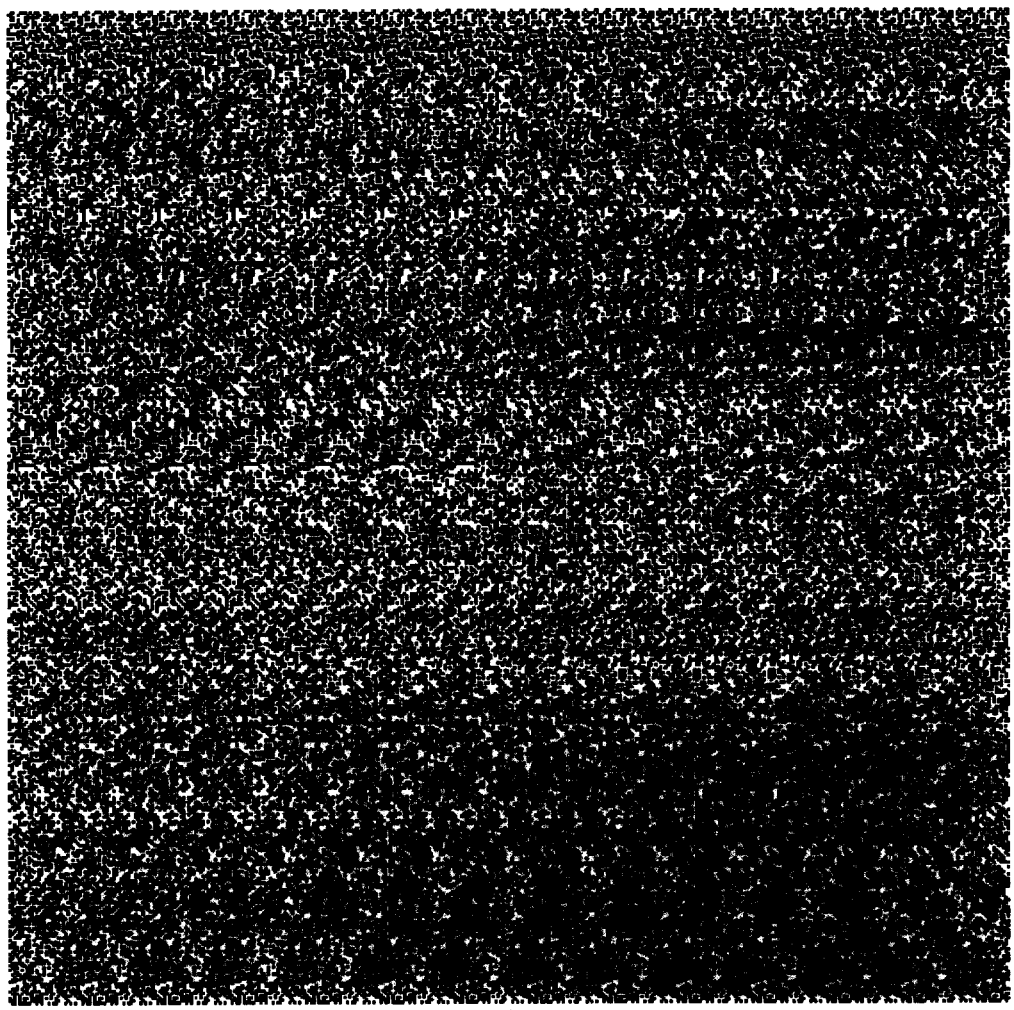

FIGURE 12 (A). *Caption on facing page.*

B. CONTOUR DEFINED BY LUMINANCE CONTRAST

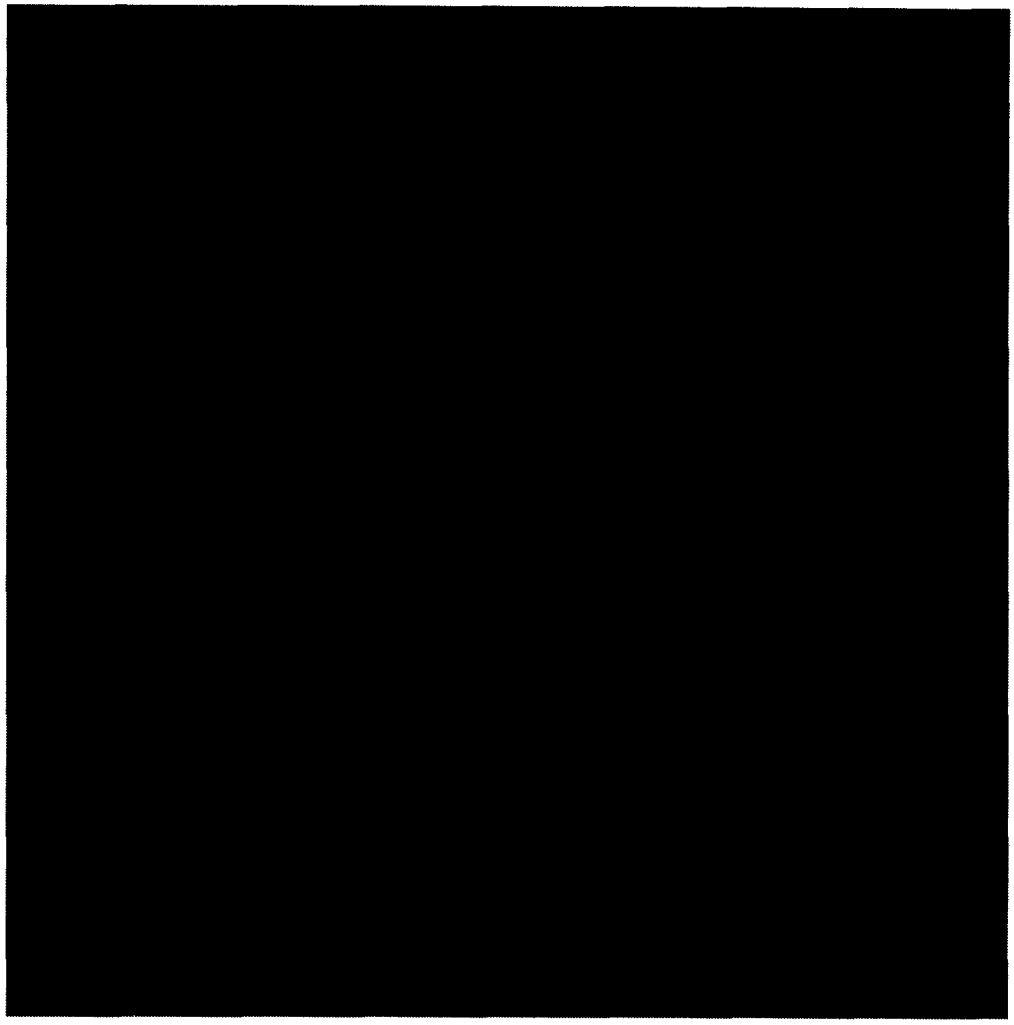

FIGURE 12. (A) Demonstration of path detection using elements defined by texture depth. The same path whose angle is 10 deg is much more detectable when the elements are defined by luminance contrast. (B) Demonstration of path detection (upper right) using elements defined by luminance contrast.

occur only when the observer is at one lateral viewing position. Lateral movement of the head will produce a path that is not aligned when projected onto the 2-D horopter. Thus, unless the binocular integration can put up with a greater degree of positional jitter, this large disparity integration will occur only when the viewing position is at a unique location. We are now taking a closer look at this problem to determine the extent to which the 3-D integration can handle such distortions.

In terms of primate neurophysiology, there is evidence for both orientationally selective (Hubel & Wiesel, 1970; Poggio & Fisher, 1977; Hawken & Parker, 1984) and orientationally unselective (Hawken & Parker, 1984) binocular neurones. It has been argued that the poor spatial localization ability of the latter would limit their role in disparity processing *per se* (Hawken & Parker, 1984). In terms of human psychophysics, it has also recently been shown that the masking of stereoscopic performance reveals two components, one that is orientationally selective and one, orientationally unselective, with its greatest magnitude at low spatial frequencies (Mansfield & Parker, 1993). Our results suggest that the outputs of disparity-selective, orientationally tuned neurones are associated to define object continuity across 3-D distances. This extends the role of orientational processes in stereopsis to beyond establishing correspondence and surface slant (Jones & Malik, 1992). Our findings appear to conflict with the conclusions of Akerstrom and Todd (1988) who showed that orientational processes do not play a strong role in stereoscopic transparency. Stereoscopic transparency represents the situation where contour integration within a depth plane is stronger than across depth planes. Stereoscopic transparency is best achieved under conditions of large inter-element separations which may prohibit local object continuity across depth. When considered in terms of the "association field" of Field *et al.* (1993) it is not surprising that orientation is ineffective at such large inter-elements distances.

If all the cortical neurones are binocular to some degree then there need be only one topological map from which such long range connections or associations are derived. However if under monocular viewing, purely monocular cells are activated, then a quite separate connectivity is required to satisfy both the 2-D and 3-D cases (e.g. see Julesz, 1971, pp. 94–95). Whether there is a separate monocular association field is indeterminate from the present results.

An issue not addressed in the present study is whether the outputs of "purely" disparity-selective cells exhibit similar rules for contour extraction. All of our stimuli had orientations defined by monocular luminance information which would have powerfully activated orientationally tuned cortical disparity cells. Julesz (1971) has elegantly shown that depth-modulated form information can be seen in random-dot stereograms where there is no corresponding monocular form information. In this situation orientation is defined by depth texture rather than luminance contrast. Do similar continuity rules exist for element paths where element orientation is defined by disparity texture? Figure 11(A) provides a demonstration of path detection in the presence of a field of background elements presented as an autostereogram in which the individual elements are not defined by monocular luminance contrast but by depth texture. The luminance contrast version of the same stimulus is seen in Fig. 11 (B). The presence of the path is not readily detected in the autostereogram although, given enough time for visual search, its presence can be deduced. Compare this to the instantaneous detection in the luminance contrast case. The inability of the cyclopean form processor to integrate across contours may be the underlying reason why it is also blind to certain textures (Nothdurft, 1985). This is of course only a demonstration and there may be special conditions where cyclopean path continuity is possible. It is, however, simply surprising that, given the detectability of the depth defined elements, their linking into a perceptual path is so weak. This may suggest that the way in which the outputs of neurones are associated to define object continuity may depend on whether those objects are themselves defined by luminance or disparity contrast.

In summary, contour integration of luminance defined elements operates over relatively large disparities and is subserved by binocular and orientationally tuned mechanisms. Different integration rules are likely for elements defined by texture depth.

REFERENCES

Akerstrom, R. A. (1988). The perception of stereoscopic transparency. *Perception & Psychophysics, 44*, 421–432.

Field, D. J., Hayes, A. & Hess, R. F. (1995). Polarity and symmetry in contour integration. *Vision Research*. Submitted.

Field, D. J., Hayes, A. & Hess, R. F. (1993). Contour integration by the human visual system; evidence for a local "association field". *Vision Research, 33*, 173–193.

Gillam, B., Chambers, D. & Russo, T. (1988). Postfusional latency in stereoscopic slant perception and the primitives of stereopsis. *Journal of Experimental Psychology: Human Perception and Performance, 14*, 163–175.

Hawken, M. J. & Parker, A. J. (1984). Contrast sensitivity and orientation selectivity in laminar iv of the striate cortex of old world monkeys. *Experimental Brain Research, 54*, 367–373.

Hubel, D. H. & Wiesel, T. N. (1970). Cells sensitive to binocular density in area 18 of the macaque monkey cortex. *Nature, 225*, 41–42.

Jones, D. G. & Malik, J. (1992). Determining three-dimensional shape from orientation and spatial frequency disparities. *Proceedings of the European Conference on Computer Vision*, May, pp. 661–669.

Julesz, B. (1971). *Foundations of cyclopean perception*. Chicago, Ill.: University of Chicago Press.

Kovacs, I. & Julesz, B. (1993). A closed curve is much more than an incomplete one: Effect of closure in completion of segmented contours. *Proceedings of the National Academy of Science, 90*, 7495–7497.

Mansfield, J. S. & Parker, A. J. (1993). An orientation-tuned component in the contrast making of stereopsis. *Vision Research, 33*, 1535–1544.

Mayhew, J. E. & Frisby, J. P. (1978). Stereopsis masking in humans is not orientationally tuned. *Perception, 7*, 431–436.

McIlhagga, W. & Mullen, K. T. (1995). The detection of colour and luminance contours. *Vision Research*. Submitted.

Northdurft, H. C. (1985). Texture discrimination does not occur at the cyclopean retina. *Perception, 14*, 527–537.

Poggio, G. F. & Fisher, B. (1977). Binocular integration and depth sensitivity in striate and prestriate cortex of behaving monkey. *Journal of Neurophysiology, 40*, 1392–1405.

Polat, U. & Sagi, D. (1993). Lateral interactions between spatial frequency channels. *Vision Research, 33*, 993–999.

Watamaniuk, S. N. J., McKee, S. P. & Grzywacz, N. M. (1995). Detecting a trajectory embedded in random-direction motion noise. *Vision Research, 35*, 65–77.

Zucker, S., Dobbins, A. & Iverson, L. (1989). Two-stages of curve detection suggest two styles of visual computation. *Neural Computation, 1*, 68–81.

Acknowledgements—This work was supported by a grant from the Medical Research Council of Canada (No. mt 10818). We are grateful to William McIlhagga and Eric Fredericksen.

APPENDIX

Stimulus Parameters

Element parameters

Gabor wavelength	10.4 or 31.2 min arc (carrier spatial wavelength)
Envelope space constant	5.2 or 15.6 min arc (Gaussian standard deviation)
Carrier phase	0 (sine phase)
Element contrast	35%
Element size	22.75 min arc

Display parameters

Cell size	31.2 min arc
# of cell rows	8
# of cell columns	8
Stereo-image pair displacement	325 min arc (from left top of left image to left top of right image)
Maximum disparity	0–12.8 min arc (spatial frequency = 5.8 c/deg) 0–38.4 min arc (spatial frequency = 1.9 c/deg)
Path length	6 (No. of elements in path)
Path_step size	37.7 min arc (length of each path step)
Step size jitter	6.5 min arc (variability of path step)
Path_angle jitter	10 deg (variability of 2-D angle of path backbone)
Element_angle jitter	10, 10 deg (variability of off-path angle)
Depth_trend	0 (starting depth value added to each successive path element)
Depth_sequence (5.8 c/deg)	Depth of each successive path element, cyclically assigned 0,0 +3.2, −3.2 min arc +6.4, −6.4 min arc +9.7, −9.7 min arc +12.8, −12.8 min arc
Depth_sequence (1.9 c/deg)	0,0 +9.6, −9.6 min arc +19.2, −19.2 min arc +29.1, −29.1 min arc +38.4, −38.4 min arc
Depth_jitter (5.8 c/deg)	Variability about the depth sequence for each path element 0 ±1.3 min arc ±2.6 min arc ±3.9 min arc ±5.2 min arc
Depth_jitter (1.9 c/deg)	0 ±3.9 min arc ±7.8 min arc ±11.7 min arc ±15.6 min arc